An Immunogold Single Extracellular Vesicular RNA and Protein (^{Au}SERP) Biochip to Predict Responses to Immunotherapy in Non-Small Cell Lung Cancer Patients

Luong T. H. Nguyen[1†], Jingjing Zhang[1†], Xilal Y. Rima[1†], Xinyu Wang[1], Kwang Joo Kwak[2], Tamio Okimoto[3], Joseph Amann[3], Min Jin Yoon[1], Takehito Shukuya[3,4], Chi-Ling Chiang,[1] Nicole Walters[1], Yifan Ma[1], Donald Belcher[1], Hong Li[1], Andre F. Palmer[1], David P. Carbone[3], L. James Lee[1,2], Eduardo Reátegui[1,3*]

[1] William G. Lowrie Department of Chemical and Biomolecular Engineering, The Ohio State University; Columbus, OH 43210, USA.

[2] Spot Biosystems Ltd.; Palo Alto, CA 94301, USA.

[3] Comprehensive Cancer Center, The Ohio State University; Columbus, OH 43210, USA.

[4] Department of Respiratory Medicine, Juntendo University; Tokyo, Japan.

[†]The authors contributed equally to this work

*Corresponding author: **reategui.8@osu.edu**

Table of Contents

SUPPORTING INFORMATION

Isolation and activation of T cells

15 mL of blood was collected in a BD Vacutainer Plastic Blood Collection Tube with K_2EDTA (#366643, Becton Dickinson, Franklin Lakes, NJ) and lysed with red blood cell lysis buffer (150 mM ammonium chloride, 10 mM sodium bicarbonate, 0.1 mM EDTA, pH = 7.4) for 5 min at room temperature (RT). After centrifugation, a pellet was resuspended in phosphate buffer saline (PBS) and T cells were isolated using an immunomagnetic negative selection kit (EasySep Human CD8+ T Cell Enrichment Kit, #19053, Stemcell Technologies, Vancouver, Canada) according to the manufacturer's instructions. The cells were subsequently activated with ImmunoCult Human CD3/CD28 T Cell Activator (1:40 dilution, #10971, Stemcell Technologies) and Interleukin 2 (10ng/mL, Human Recombinant IL-2 (CHO-expressed), Stemcell Technologies) in 6 mL of a serum-free and xeno-free medium (ImmunoCult-XF T Cell Expansion Medium, Stemcell Technologies) for 3 days at an initial concentration of 10^6 cells/mL to stimulate PD-1 expression. After incubation, the culture was centrifuged at 2000 × g for 10 min to remove suspended cells and cell debris before EV purification.

Immunofluorescence staining of cells

H1568 cells grown on a glass slide in 16-well chambers were first fixed in a 4% formaldehyde solution in PBS for 15 min. Non-specific bindings were blocked with 3% (w/v) bovine serum albumin (BSA) and 0.05% (v/v) Tween 20 in PBS for 1 h at RT. A mouse anti-CD63 monoclonal antibody (MX-49.129.5) – Alexa Fluor 488 conjugate (#sc-5275 AF488, Santa Cruz Biotechnology), a mouse anti-CD9 monoclonal antibody (C-4) – Alexa Fluor 546 conjugate (#sc-13118 AF546, Santa Cruz Biotechnology), and a rabbit anti-PD-L1 monoclonal antibody – Alexa Fluor 647 conjugate (#41726S, Cell Signaling Technology) were diluted in 1% (w/v) BSA and 0.05% (v/v) Tween 20 in PBS, and incubated with the cells for 1 hr at RT. After washing three times with PBS for 5 min each, the glass slide was detached and mounted onto a cover glass using ProLong Gold Antifade Mountant with DAPI. The images were taken with a confocal microscope (Olympus FV3000).

EV imaging with flow cytometry

Purified EVs from IFN-γ-stimulated H1568 cells, non-stimulated H1568 cells, MEF, and activated T cells were stained with CD63 (sc-5275 AF488, Santa Cruz Biotechnology) and CD9 (sc-59140, Santa Cruz Biotechnology) antibodies in a 1% (w/v) BSA solution overnight at 4°C. To examine PD-L1 specificity, EVs from IFN-γ-stimulated H1568 cells, non-stimulated H1568 cells, and MEF were stained with a PD-L1 (Rabbit mAb #86744, Cell Signaling Technology) antibody in a 1% (w/v) BSA solution overnight at 4°C. As for PD-1, EVs from activated T cells and MEF were stained with a PD-1 (mAb #53-9969-42, Invitrogen) antibody in a 1% (w/v) BSA solution overnight at 4°C. For mRNA detection, PD-L1 and PD-1 MBs were incubated in 1× tris EDTA for 2 hr at 37°C. PBS was utilized as the negative control. EVs were then imaged using ImageStream^X mark II.

Western blot

EVs from IFN-γ-stimulated H1568 cells, non-stimulated H1568 cells, MEF, and activated T cells were first isolated and enriched using TFF. All samples were then concentrated via the Total Exosome Isolation Kit (ThermoFisher Scientific) according to the manufacturer's protocol. The total protein extracted from EV and cell lysates was quantified using the Pierce® BCA Protein Assay Kit (ThermoFisher Scientific), where 20 µg of the total protein for each sample was loaded into a sodium dodecyl sulfate-polyacrylamide gel for electrophoresis. The separated proteins were transferred onto 0.2-µm nitrocellulose membranes (Bio-Rad Laboratories), where primary antibodies against CD63 (ab231975, Abcam), CD9 (MA1-19301, ThermoFisher Scientific), PD-1 (86163T, Cell Signaling Technology), and PD-L1 (13684T, Cell Signaling Technology) were utilized. Later, horseradish peroxidase-conjugated goat anti-rabbit (Abcam) or goat anti-mouse IgG (Abcam) was added as secondary antibodies and were subsequently imaged.

Viral detection

Moloney murine leukemia viruses (MV-M-V5, ViroFlow Technologies, Ontario, CA) were captured with ^{Au}SERP via a V5 capture antibody (ab-9116, Abcam) and detected with a V5 antibody conjugated with FITC (R963-25, Invitrogen) following the same protocol for protein detection as previously described.

Dynamic light scattering.

Size distributions were determined in purified serum diluted 10X in DI water with a Nano Zetasizer Zen3600 dynamic light scattering (Malvern Instruments Ltd., Worcestershire, United Kingdom). Briefly, the samples were illuminated at 637 nm at a 90 º angle at 22 ºC.

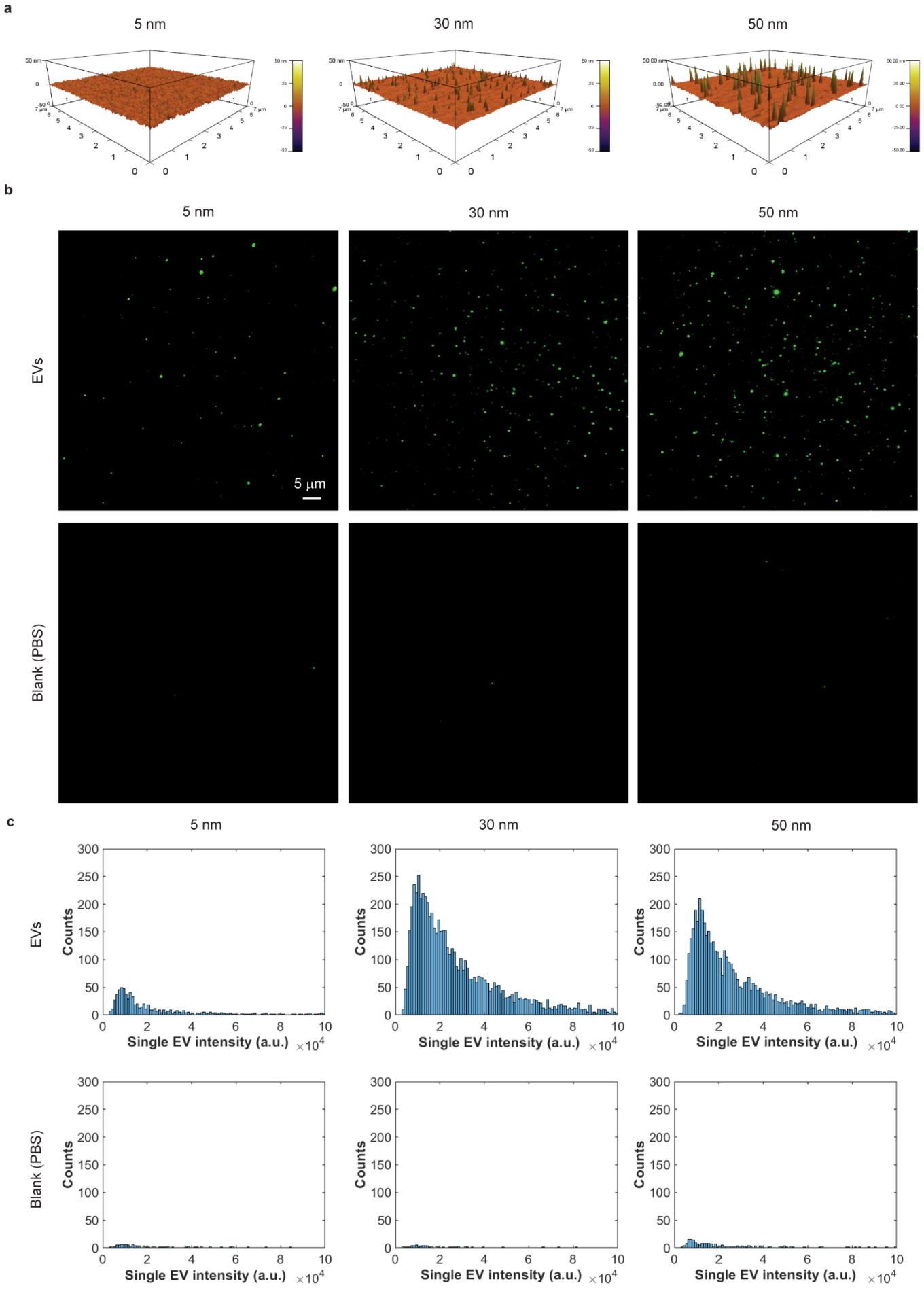
a
5 nm
30 nm
50 nm
b
5 nm
30 nm
50 nm
EVs
Blank (PBS)
5 μm
c
5 nm
30 nm
50 nm
EVs
Blank (PBS)
Counts
Single EV intensity (a.u.)
×10^4

Figure S1. Characterization of ^{Au}SERP coated with different-sized gold nanoparticles (5, 30, and 50 nm). **a** 3D height atomic force microscopy (AFM) images. **b** Representative total internal reflection fluorescence (TIRF) microscopic images of CD63 protein expression on the surface of H1568 single extracellular vesicles (EVs) in comparison with blank controls (PBS). **c** Distributions of fluorescence intensity of CD63 protein signals on single EVs. a.u., arbitrary units.

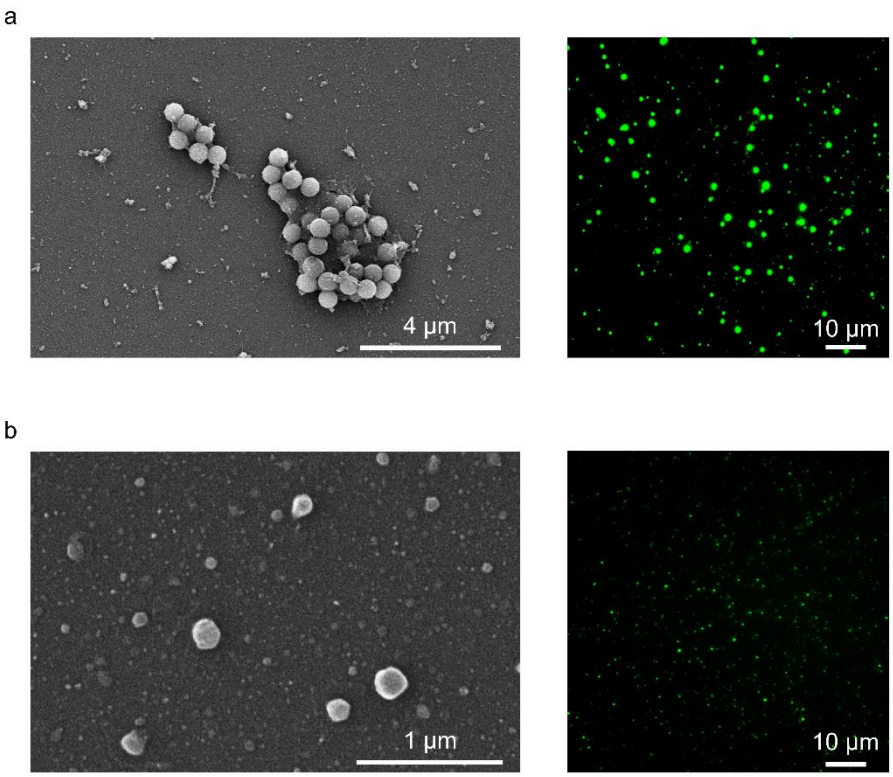

Figure S2. Morphological differences between single EVs and EV clusters. **a** EVs derived from U251 cells, a glioblastoma cell line, tend to secrete EV clusters as demonstrated by SEM, which produce large, aggregate fluorescent signals in TIRF images. **b** EVs derived from H1568 cells, an NSCLC cell line, tend to secrete single EVs as demonstrated by SEM, which produce smaller, localized fluorescent signals in TIRF images.

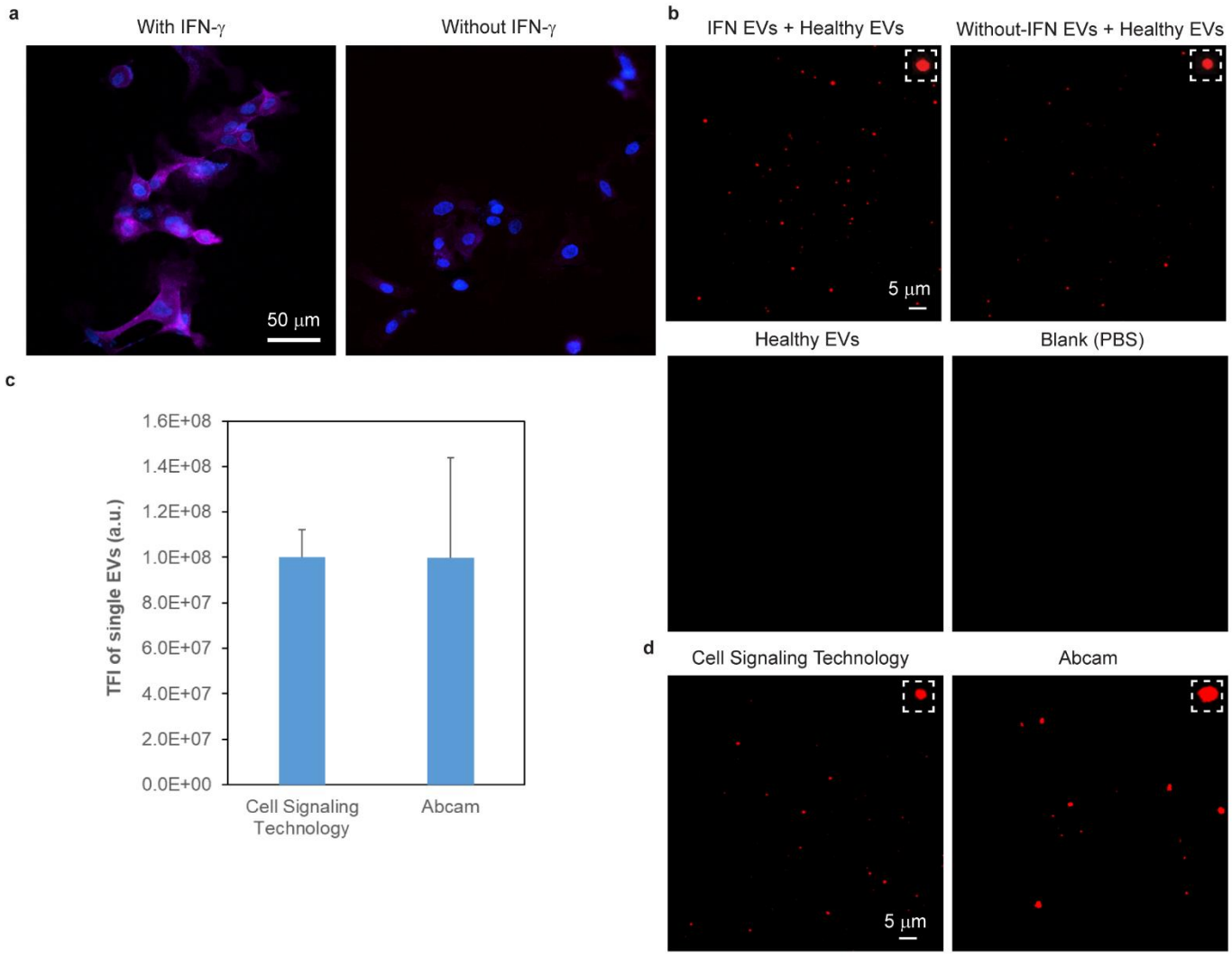

Figure S3. *In vitro* model and characterization of cellular and single-EV PD-L1 protein. **a** Immunofluorescence staining of PD-L1 protein in H1568 cells with/without interferon-gamma (IFN-γ) stimulation. Cell nuclei and PD-L1 protein were stained blue (by DAPI) and magenta (by anti-PD-L1 antibody), respectively. **b** Original TIRF microscopic images for Fig. 2c. The insets show the PD-L1 protein signals on a single EV. **c** A comparison of two different anti-PD-L1 antibodies provided by Cell Signaling Technology and Abcam to detect PD-L1 proteins on the surface of single EVs derived from IFN-γ-stimulated H1568 cells with ^{Au}SERP. The H1568 EVs were spiked in healthy donor EVs at a 1:1 ratio with 10^9 particles/mL each. The data were expressed as mean ± SD; n = 2. TFI, total fluorescence intensity; a.u., arbitrary units. **d** Representative TIRF microscopic images of PD-L1 protein expression of the H1568 single EVs stained by the two different antibodies. The insets show the PD-L1 protein signals on a single EV.

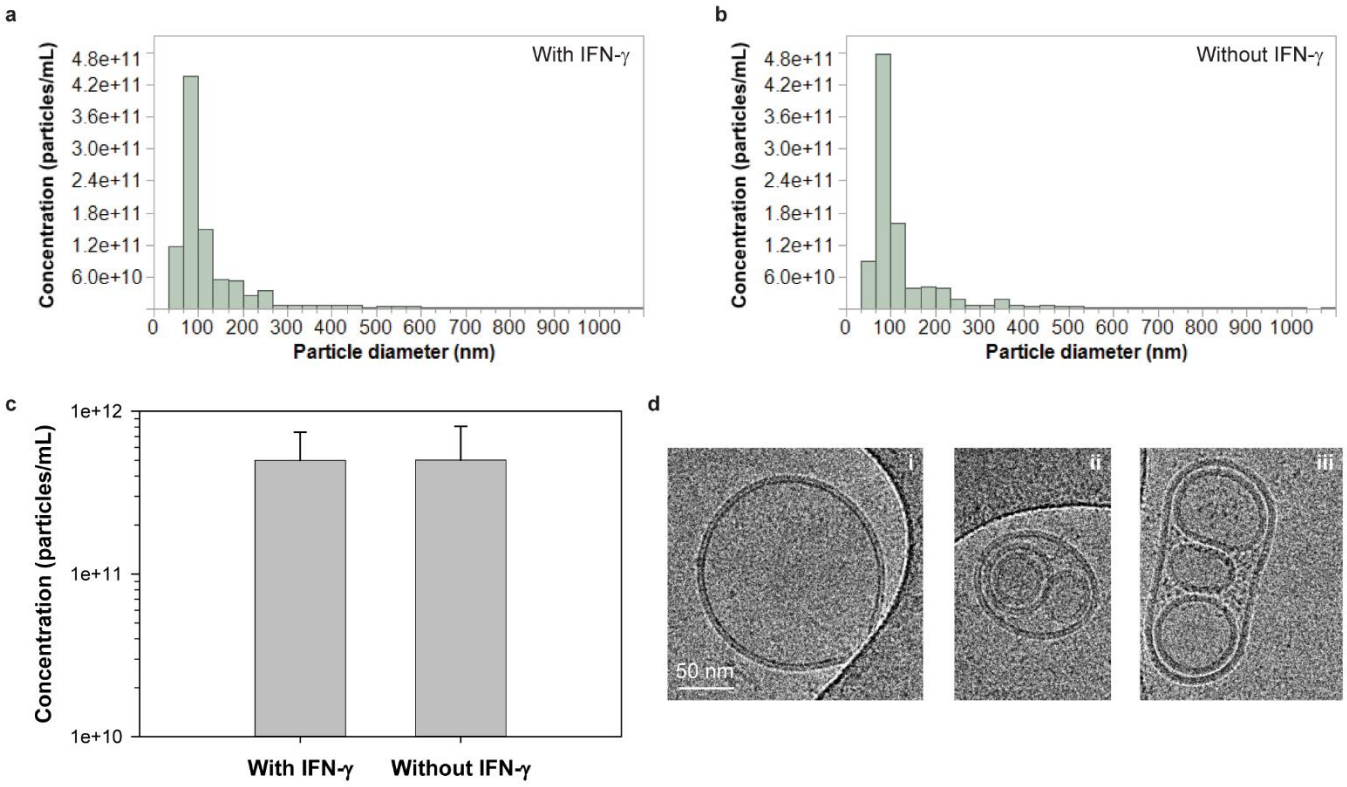

Figure S4. Size and morphological characterization of EVs produced by H1568 cells. **a-b** Size distributions of EVs derived from H1568 cells with/without IFN-γ stimulation measured with Tunable Resistive Pulse Sensing (TRPS). **c** A comparison of their EV concentrations. The data were expressed as mean ± SD; n = 3. **d** Cryo-TEM images of EVs derived from IFN-γ-stimulated H1568 cells.

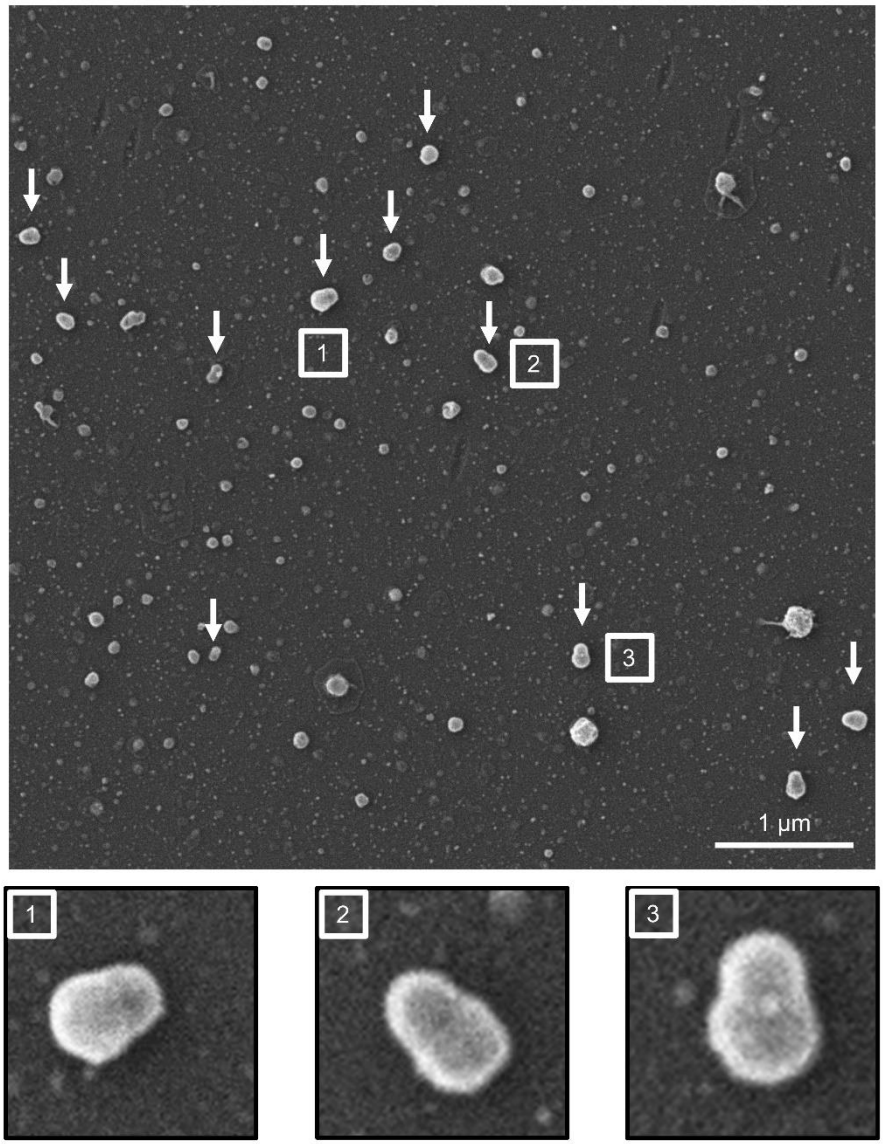

Figure S5. Large-scale SEM of single CLN-MB and single EV fusion. The arrows indicate fusion events and the numbers correspond to the enlarged panels at the bottom.

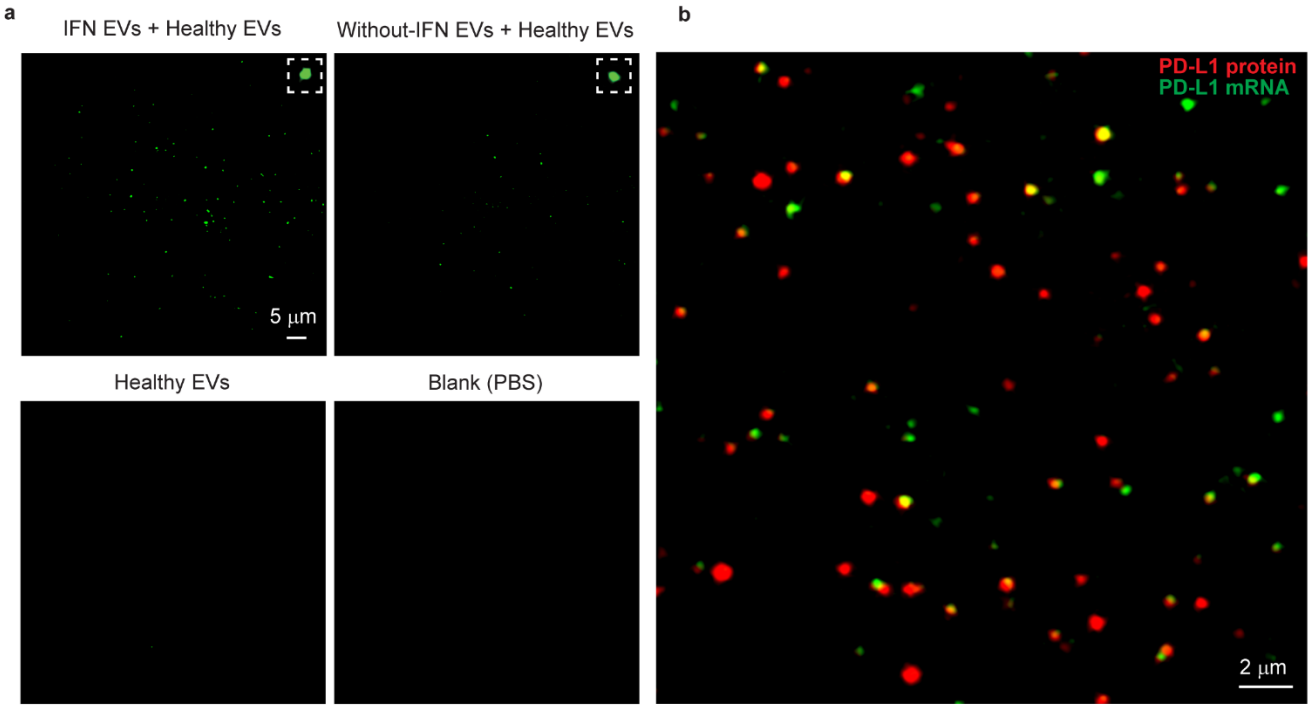

Figure S6. *In vitro* model and characterization of single-EV PD-L1 protein and mRNA with ^{Au}SERP**. a** Original TIRF microscopic images for Fig. 3e. The insets show the PD-L1 mRNA signals on a single EV. **b** Multiplex imaging of PD-L1 protein and mRNA from single EVs derived from IFN-γ-stimulated H1568 cells. PD-L1 protein and mRNA were stained green and red, respectively. The colocalized single-EV PD-L1 protein and mRNA signals appear yellow.

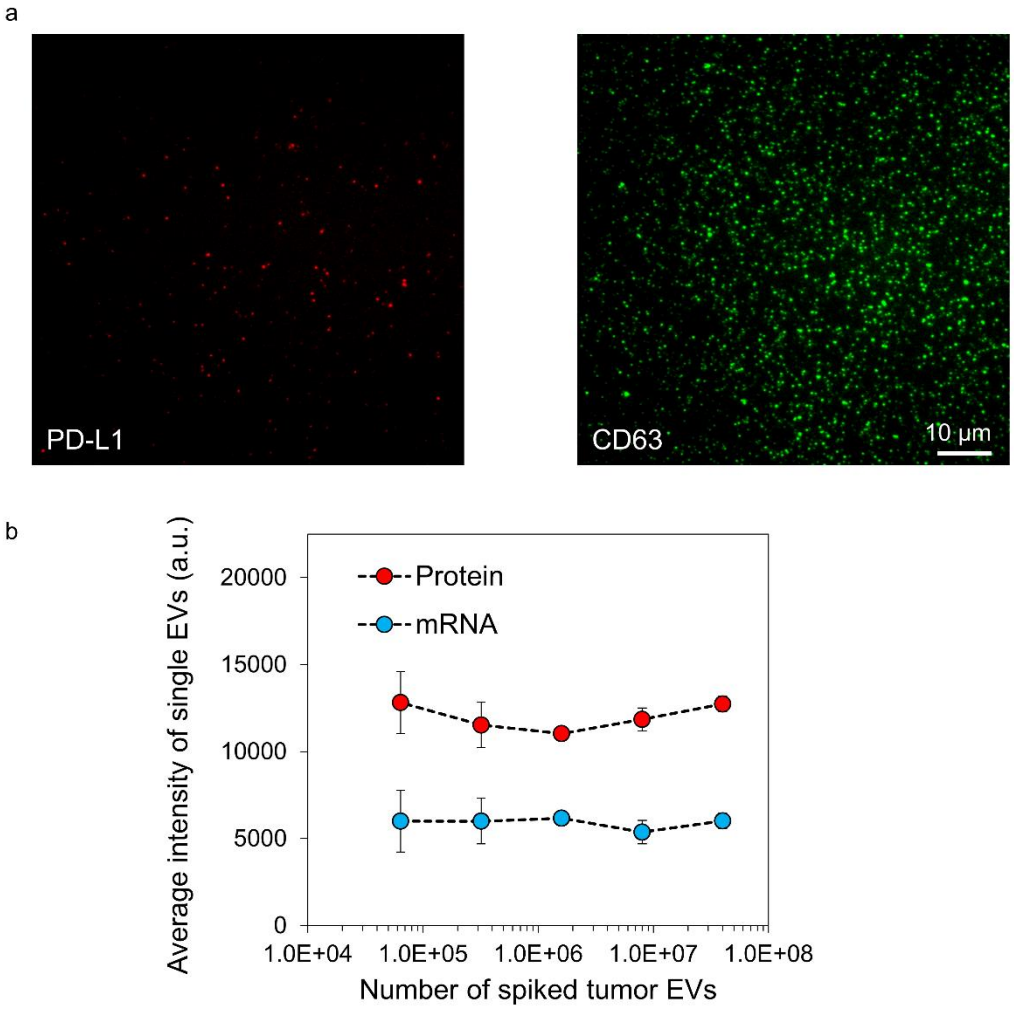

Figure S7. Upper limit and linear range of ^{Au}SERP. **a** Upper limit of single-vesicle detection for ^{Au}SERP. EVs spiked into healthy donor EVs derived from IFN-γ-stimulated H1568 cells at a concentration of 10^{11} particles/mL, demonstrated the saturation of the ^{Au}SERP biochip surface and aggregation of EVs as shown by detecting CD63 (right), which is not clearly represented by the low abundance biomarker, PD-L1 (left). **b** The average intensities of the histogram for various concentrations of spiked tumor EVs. The data were expressed as mean ± SD; n = 2. a.u., arbitrary units.

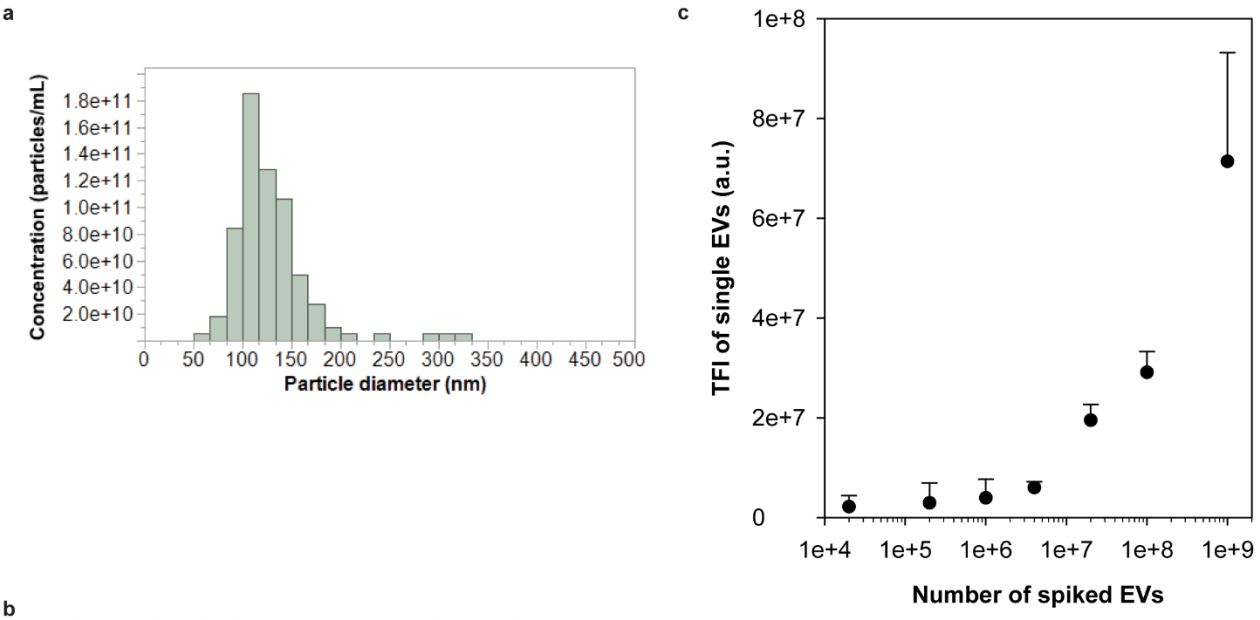
a
Concentration (particles/mL)
1.8e+11
1.6e+11
1.4e+11
1.2e+11
1.0e+11
8.0e+10
6.0e+10
4.0e+10
2.0e+10
0 50 100 150 200 250 300 350 400 450 500
Particle diameter (nm)
c
TFI of single EVs (a.u.)
1e+8
8e+7
6e+7
4e+7
2e+7
0
1e+4 1e+5 1e+6 1e+7 1e+8 1e+9
Number of spiked EVs

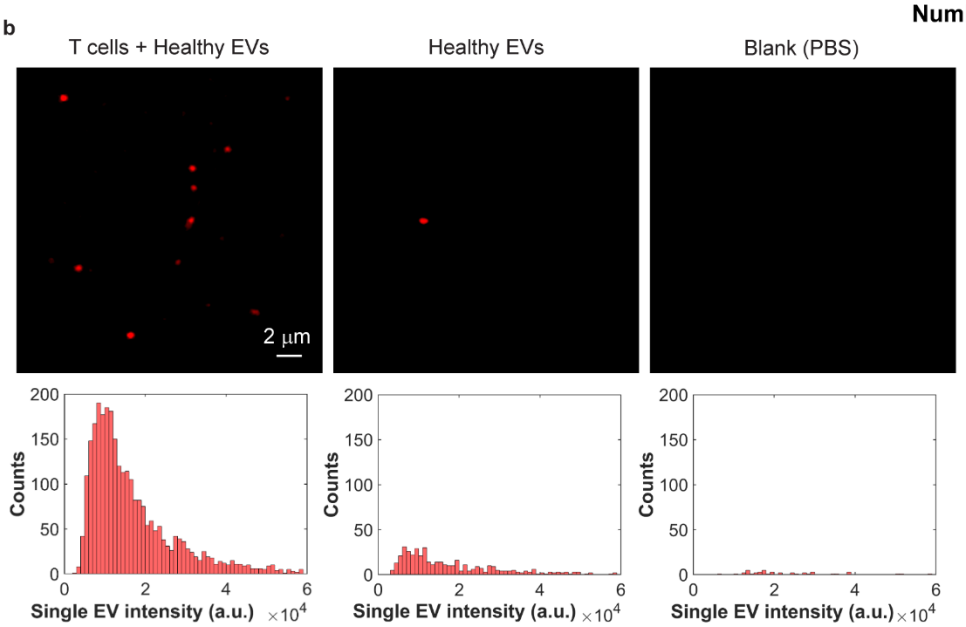
b
T cells + Healthy EVs
Healthy EVs
Blank (PBS)
2 μm
Counts
Single EV intensity (a.u.) ×10^4

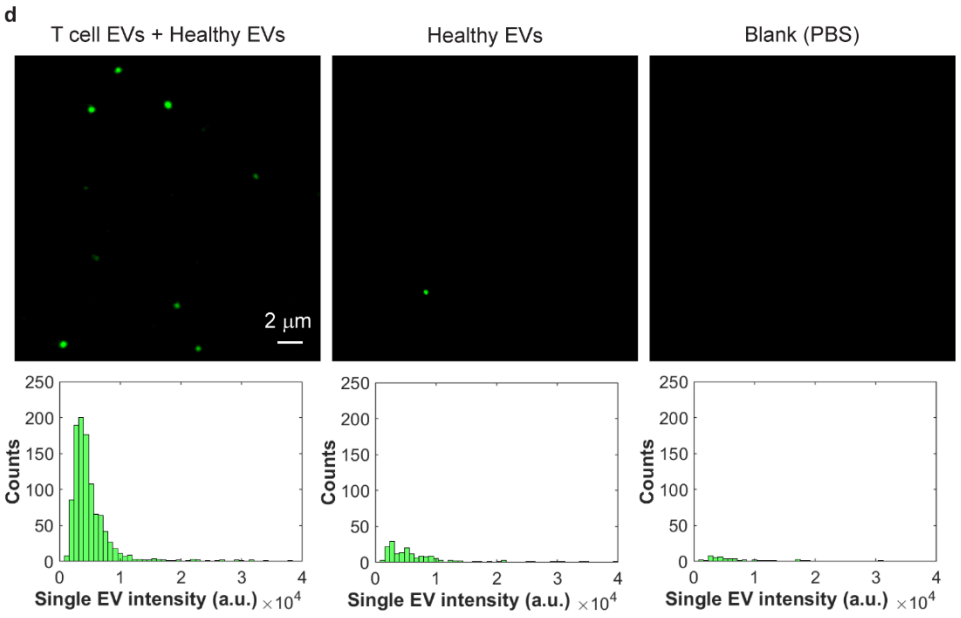
d
T cell EVs + Healthy EVs
Healthy EVs
Blank (PBS)
2 μm
Counts
Single EV intensity (a.u.) ×10^4

Figure S8. *In vitro* model and characterization of single-EV PD-1 protein and mRNA. **a** The size distribution of EVs produced by activated T cells measured with TRPS. **b** Representative TIRF microscopic images and their corresponding histograms of PD-1 protein expression on the surface of single EVs derived from activated T cells in comparison with negative controls. The single-EV PD-1 protein signals were characterized with ^{Au}SERP using an anti-PD-1 antibody and the TSA method. T cell-derived EVs were spiked in healthy donor EVs with 5×10^{10} particles/mL each. TFI, total fluorescence intensity; a.u., arbitrary units. **c** Quantitative detection of PD-1 protein with ^{Au}SERP. T cell-derived EVs were spiked in healthy donor EVs at different concentrations ranging from 0 to 5×10^{10} particles/mL, while the healthy donor EV concentration was kept constant at 5×10^{10} EVs/mL. The limit of detection (LOD) of ^{Au}SERP for PD-1 protein was ~ 10^6 spiked T cell EVs. The data were expressed as mean ± SD; n = 3. **d** Representative TIRF microscopic images and their corresponding histograms of PD-1 mRNA in single EVs derived from activated T cells in comparison with negative controls. The single-EV PD-1 mRNA signals were characterized with ^{Au}SERP using PD-1 CLN-MBs. T cell-derived EVs were spiked in healthy donor EVs with 5×10^{10} particles/mL each.

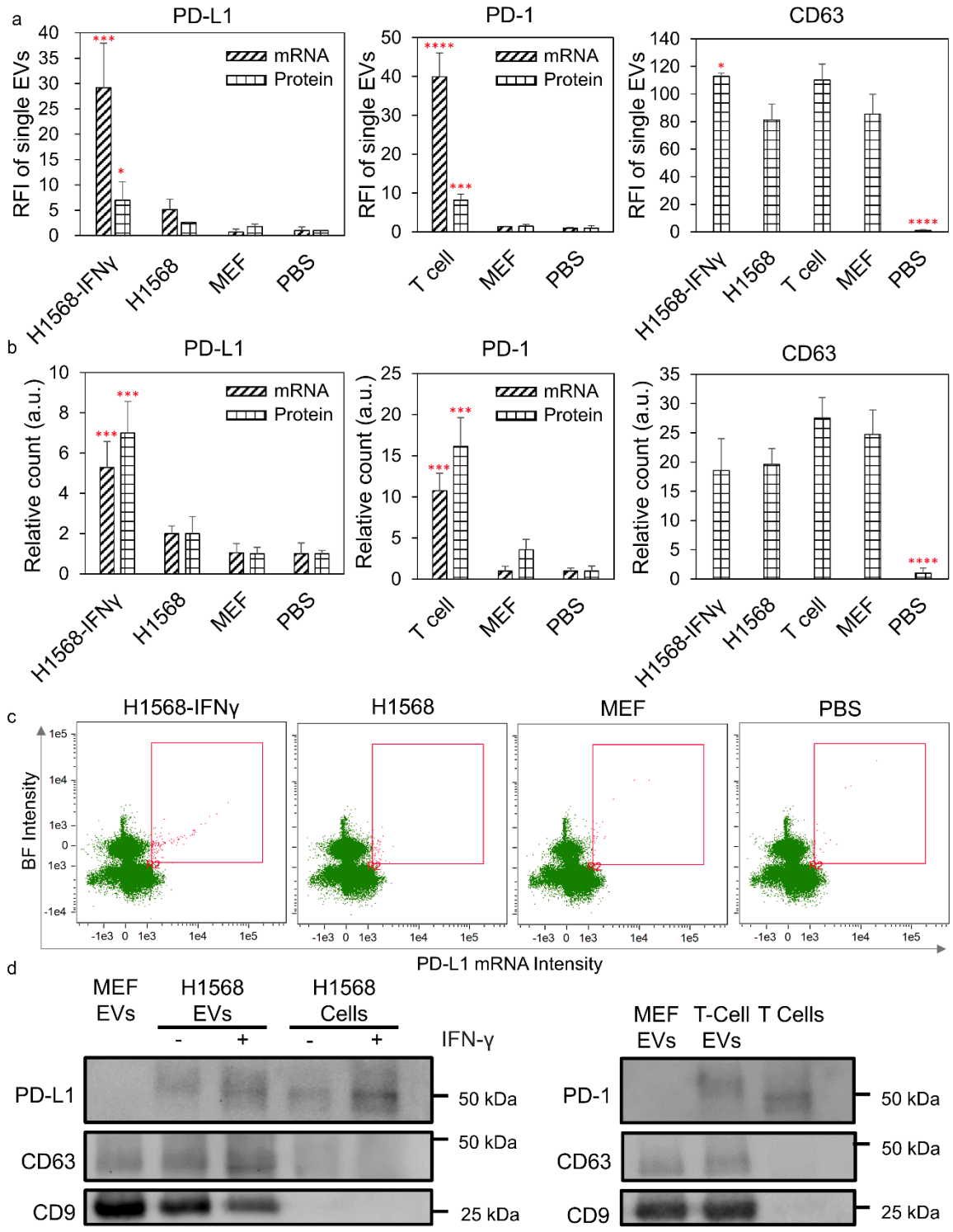

Figure S9. Specificity of ^{Au}SERP probes to PD-L1^{+}/PD-1^{+} EVs. **a** Quantitative fluorescence intensities of PD-L1/PD-1 protein and mRNA and CD63 protein expression levels on EVs derived from IFN-γ-stimulated H1568 cells, non-stimulated H1568 cells, activated T cells, and mouse embryonic fibroblasts (MEF, negative control for PD-L1/PD-1) as measured by ^{Au}SERP (*p < 0.05, ***p < 0.001, ****p < 0.0001, Tukey's HSD test with respect to MEF). **b** Counts of PD-L1^{+}/PD-1^{+} EVs via protein and mRNA detection and CD63^{+} EVs via protein detection from EVs derived from IFN-γ-stimulated H1568 cells, non-stimulated H1568 cells,

activated T cells, and MEF as measured by high-resolution flow cytometry (***$p < 0.001$, ****$p < 0.0001$, Tukey's HSD test with respect to MEF). **c** Representative scatter plots for PD-L1 mRNA cargo via high-resolution flow cytometry. **d** Qualitative expression of PD-L1/PD-1/CD63 proteins on EVs derived from IFN-γ-stimulated H1568 cells, non-stimulated H1568 cells, activated T cells, and MEF as measured by western blot. The data were expressed as mean ± SD; n = 3. RFI, relative fluorescence intensity; a.u., arbitrary units.

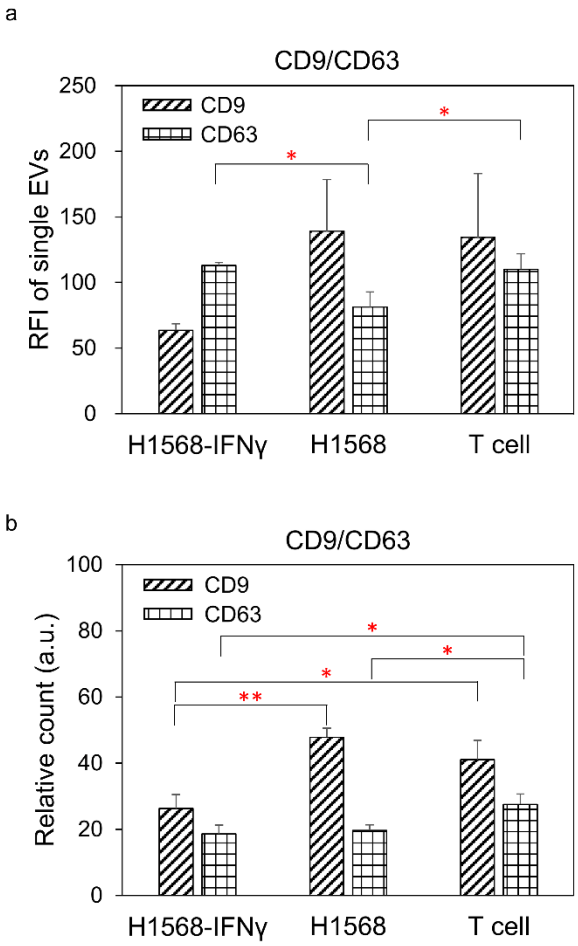

Figure S10. Expression levels of CD63/CD9 on the model EVs. **a** Quantitative fluorescence intensities of CD63/CD9 protein and mRNA expression levels on EVs derived from IFN-γ-stimulated H1568 cells, non-stimulated H1568 cells, and activated T cells as measured by ^{Au}SERP (*$p < 0.05$, Tukey's HSD test). **b** Counts of $CD63^+/CD9^+$ EVs via protein detection from EVs derived from IFN-γ-stimulated H1568 cells, non-stimulated H1568 cells, and activated T cells as measured by high-resolution flow cytometry (*$p < 0.05$, **$p < 0.01$,Tukey's HSD test). The data were expressed as mean ± SD; n = 3. RFI, relative fluorescence intensity; a.u., arbitrary units.

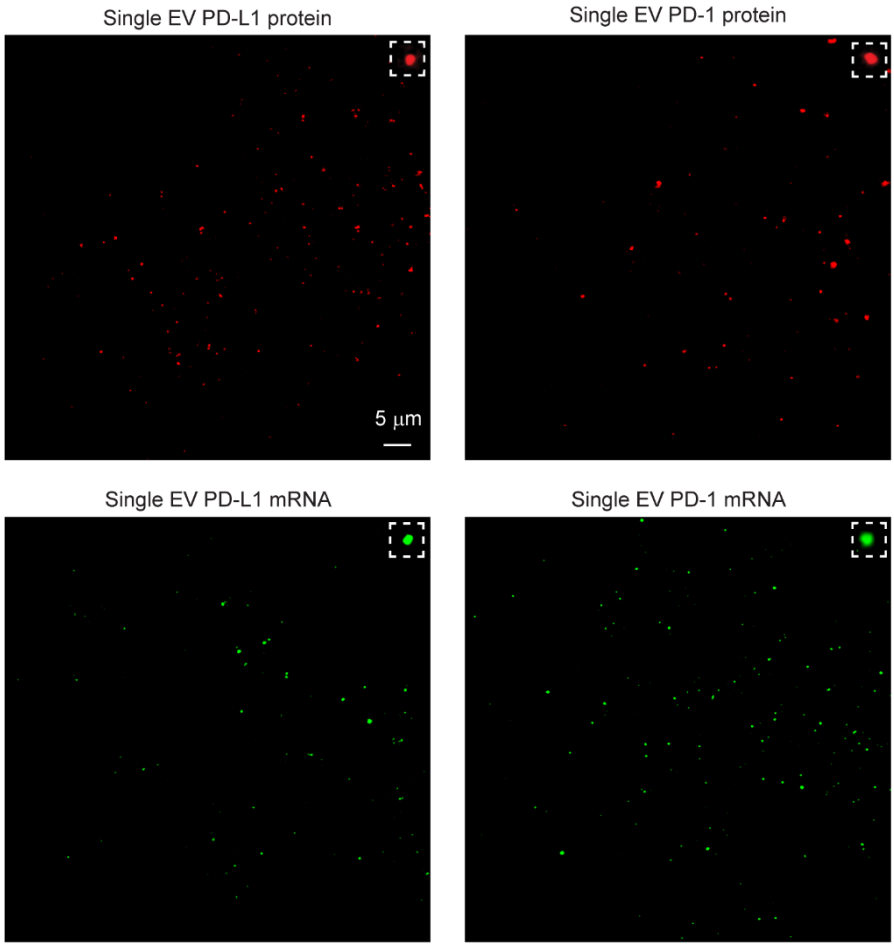

Figure S11. Original TIRF microscopic images for Fig. 4c. The insets show the PD-1/PD-L1 protein and mRNA signals on a single EV.

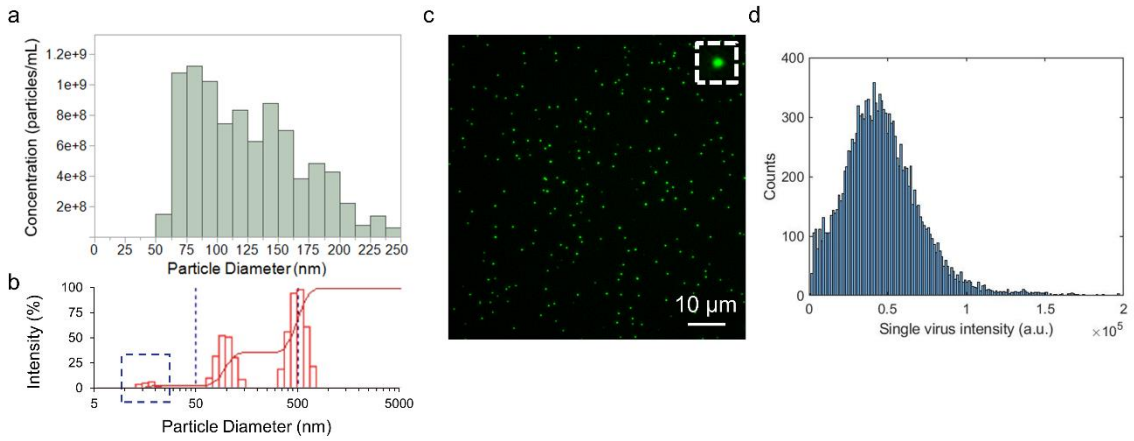

Figure S12. Viral detection with ^{Au}SERP to prove sEV detection. **a** Size distribution of sEVs from a purified serum sample. **b** Dynamic light scattering of EVs from a purified serum sample. The dotted box indicates the presence of EVs < 50 nm. **c** Moloney murine leukemia virus (MLV) was captured and detected with antibodies targeting the V5 epitope. The inset shows a single virus particle. **d** The corresponding histogram for the TIRF images.

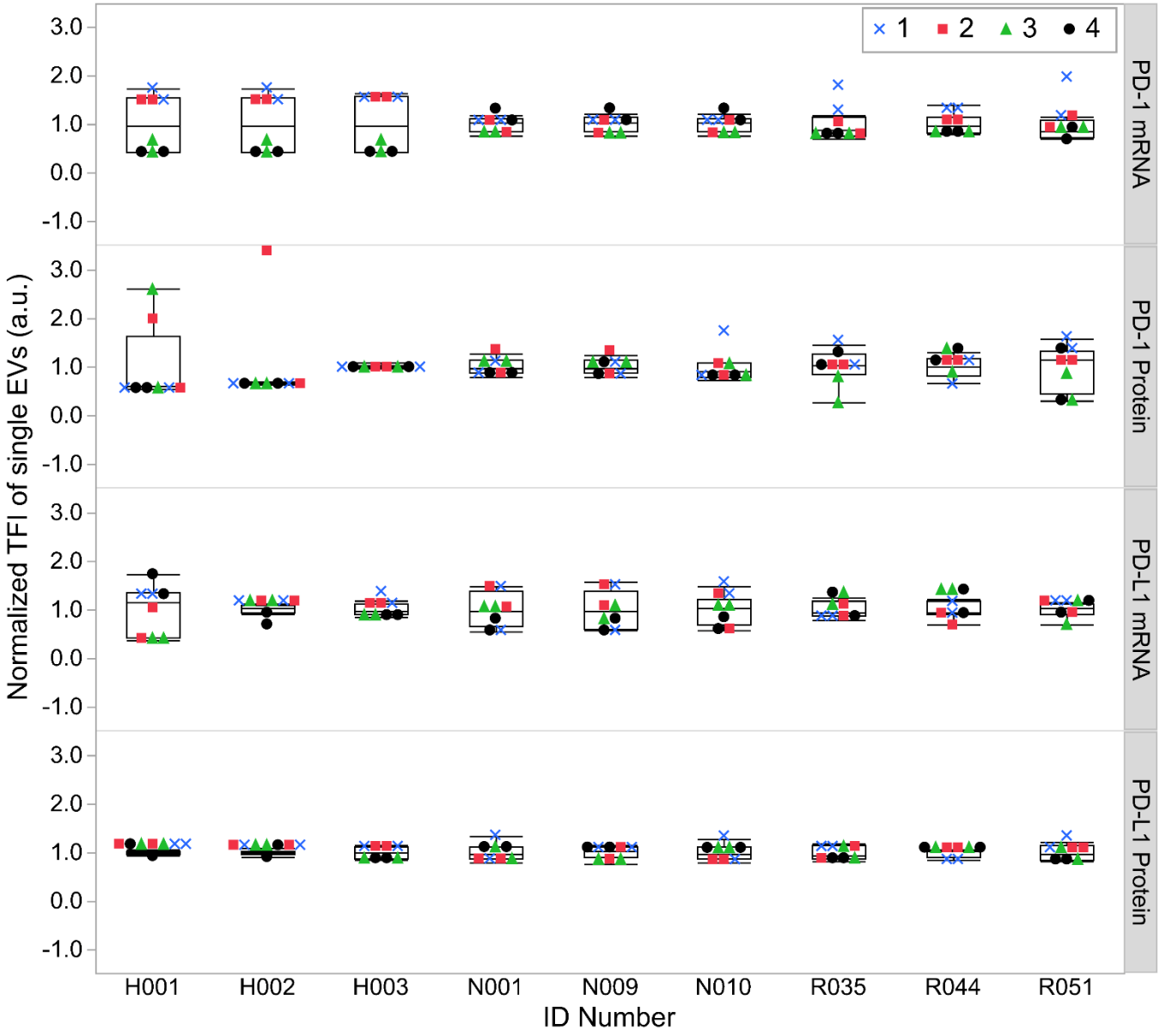

Figure S13. Repeatability of ^{Au}SERP across various serum samples for PD-L1/PD-1 protein and mRNA. Each biochip replicate is represented by a different symbol (■, ●, ▲, and ×). The TFI was normalized to the average TFI of the sample to demonstrate the coefficient of variation as the standard deviation.

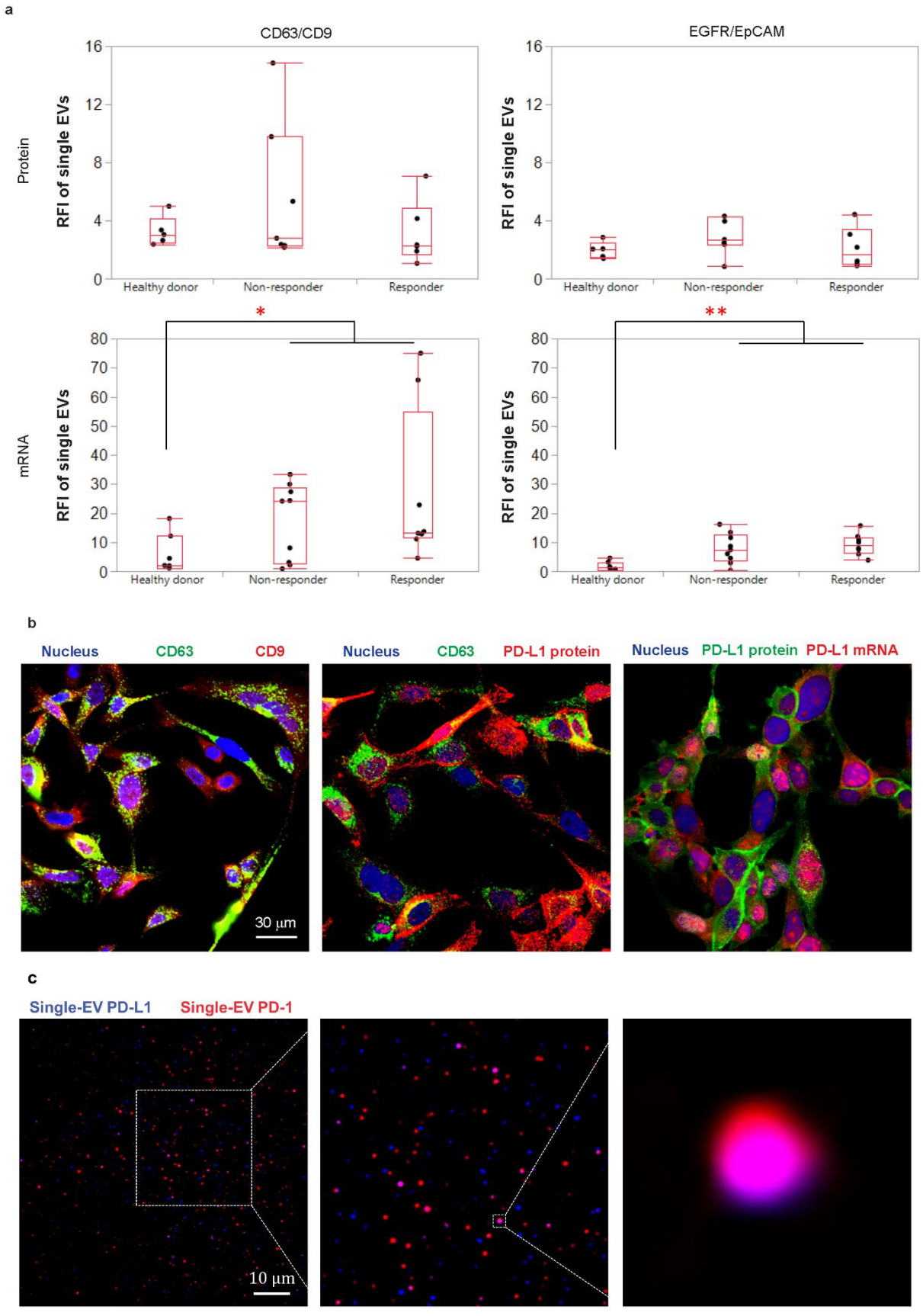

Figure S14. Single-EV PD-L1 protein and mRNA characterization in subpopulations. **a** Comparisons of two different capture antibody cocktails (anti-CD63/CD9 and anti-EGFR/EpCAM) on the measurements of PD-L1 protein and mRNA signals in single EVs isolated from the serum of healthy donors, non-responders, and

responders with ^{Au}SERP. Each antibody (anti-CD63, anti-CD9, anti-EGFR, and anti-EpCAM) was used at a concentration of 10 μg/mL. For protein characterization, a cohort including healthy donors (n = 5), non-responders (n = 7), and responders (n = 6) was tested. For mRNA characterization, a cohort including healthy donors (n = 7), non-responders (n = 9), and responders (n = 8) was tested. (*$p < 0.05$, **$p < 0.01$, Mann-Whitney *U* test). RFI, relative fluorescence intensity. **b** Confocal fluorescence microscopic images of CD63/CD9/PD-L1 proteins and PD-L1 mRNA in IFN-γ-stimulated H1568 cells. CD63/CD9/PD-L1 proteins were stained using the corresponding antibodies, while PD-L1 mRNA was visualized using PD-L1 MB via fluorescent *in situ* hybridization. Cell nuclei were stained blue using DAPI. **c** TIRF images of PD-L1 and PD-1 protein colocalization on single EVs from NSCLC patient serum.

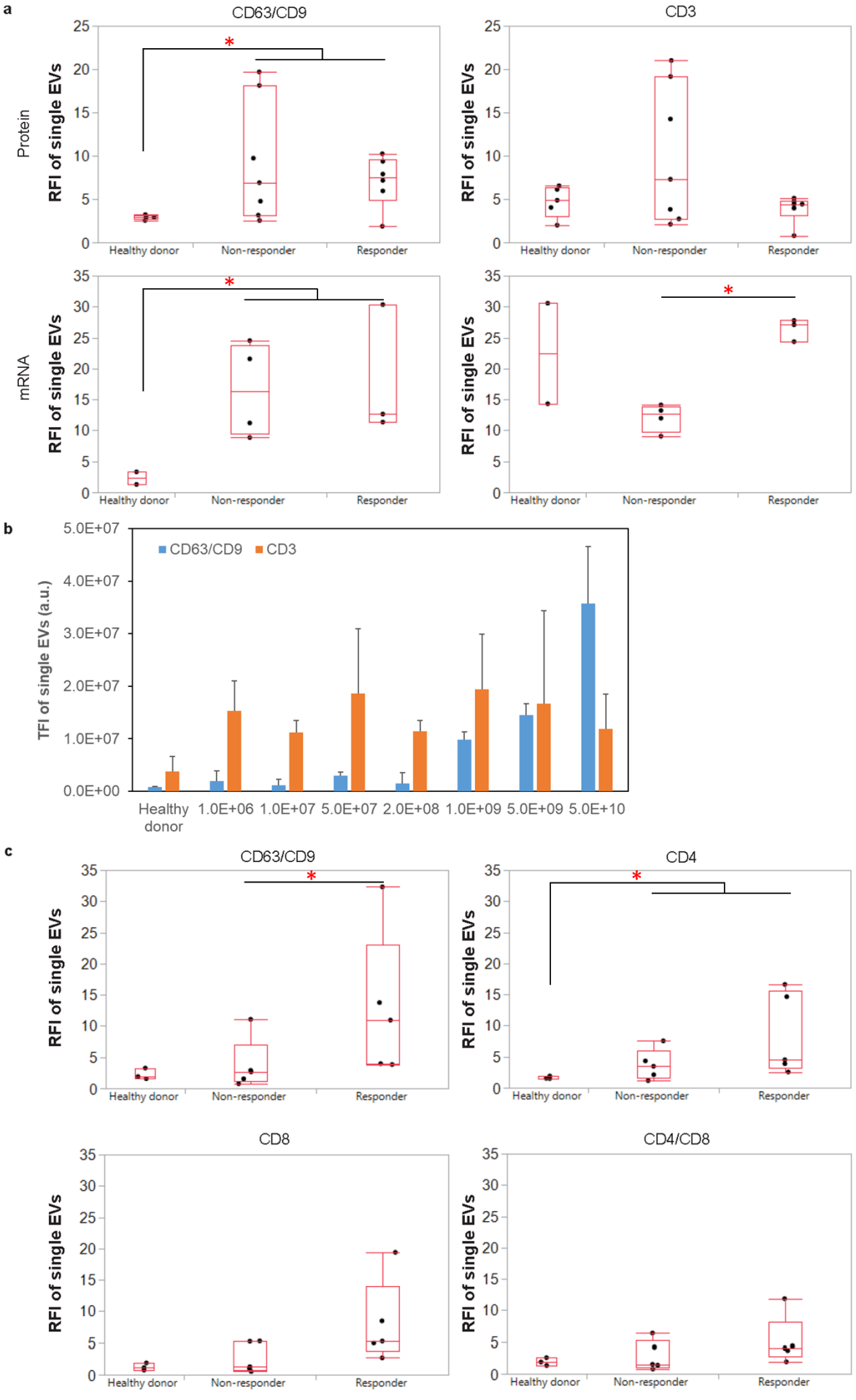
a
CD63/CD9
CD3
Protein
mRNA
RFI of single EVs
Healthy donor
Non-responder
Responder
b
CD63/CD9
CD3
TFI of single EVs (a.u.)
5.0E+07
4.0E+07
3.0E+07
2.0E+07
1.0E+07
0.0E+00
Healthy donor
1.0E+06
1.0E+07
5.0E+07
2.0E+08
1.0E+09
5.0E+09
5.0E+10
c
CD63/CD9
CD4
CD8
CD4/CD8
RFI of single EVs
Healthy donor
Non-responder
Responder

Figure S15. A comparison of different capture antibodies on the measurement of PD-1 protein and mRNA signals in single EVs with ^{Au}SERP. **a** A comparison of anti-CD63/CD9 and anti-CD3 capture antibodies on the measurement of PD-1 protein and mRNA signals in single EVs isolated from sera of healthy donors, non-responders, and responders. The cocktail of anti-CD63/CD9 antibodies was used at a concentration of 10 μg/mL each, while the anti-CD3 antibody was used at 20 μg/mL. For protein characterization, a cohort including healthy donors (n = 5), non-responders (n = 7), and responders (n = 6) was tested. For mRNA characterization, a cohort including healthy donors (n = 2), non-responders (n = 4), and responders (n = 3) was tested. (*$p < 0.05$, Mann-Whitney *U* test). RFI, relative fluorescence intensity. **b** Quantitative detection of PD-1 protein with different capture antibodies (anti-CD63/CD9 and anti-CD3). T cell-derived EVs were spiked in healthy donor EVs at different concentrations ranging from 0 to 5×10^{10} particles/mL, while the healthy donor EV concentration was kept constant at 5×10^{10} EVs/mL. TFI, total fluorescence intensity; a.u., arbitrary units. **c** A comparison of different capture antibodies (anti-CD63/CD9, anti-CD4, anti-CD8, and anti-CD4/CD8) on the measurement of PD-1 protein on the surface of single EVs isolated from the serum of healthy donors (n = 3), non-responders (n = 5), and responders (n = 5). The cocktail of anti-CD63/CD9 and anti-CD4/CD8 antibodies were both used at a concentration of 10 μg/mL for each antibody, while single anti-CD4 and anti-CD8 antibodies were used at 20 μg/mL. (*$p < 0.05$, Mann-Whitney *U* test). RFI, relative fluorescence intensity.

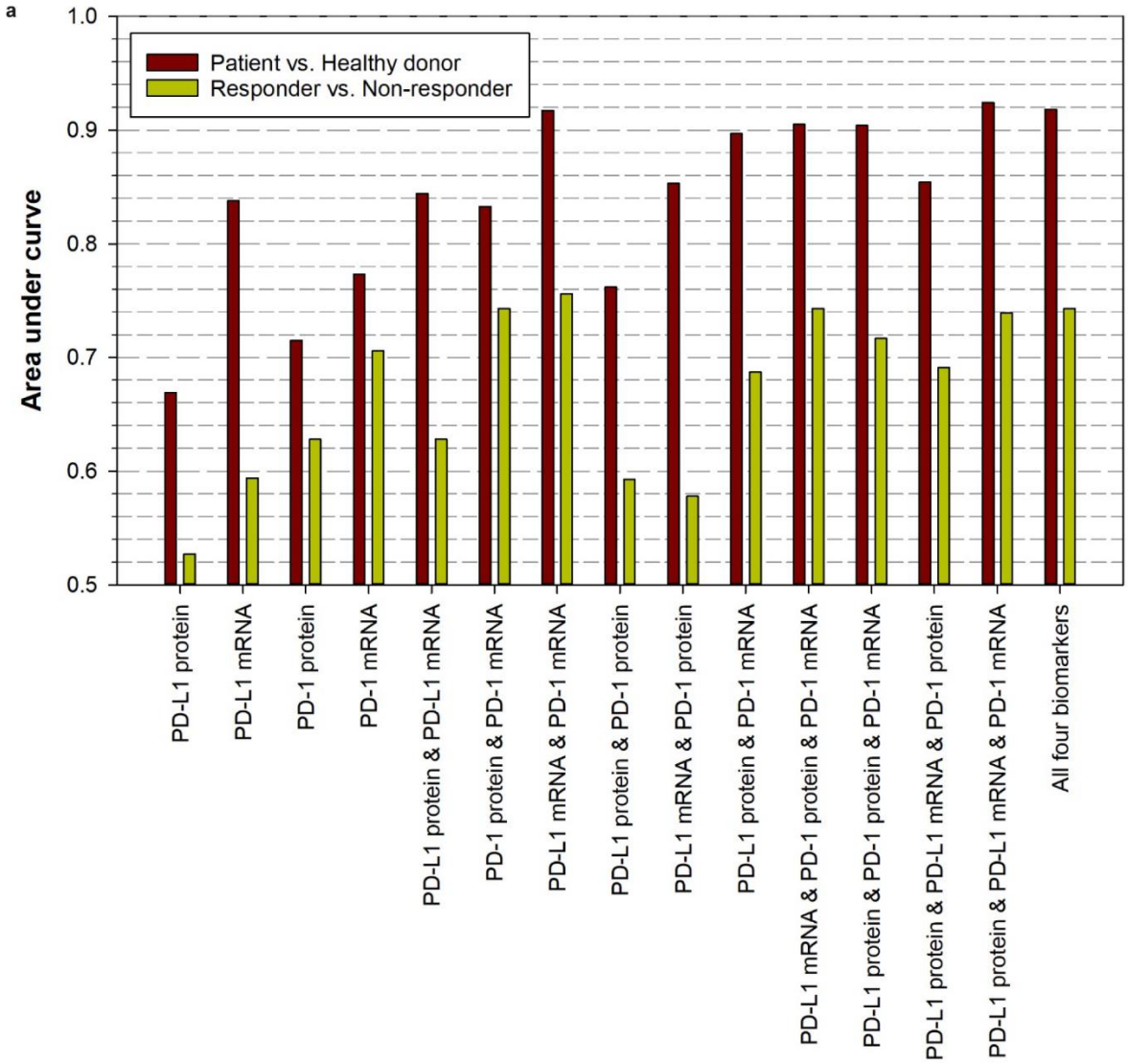
a
Patient vs. Healthy donor
Responder vs. Non-responder
Area under curve
1.0
0.9
0.8
0.7
0.6
0.5
PD-L1 protein
PD-L1 mRNA
PD-1 protein
PD-1 mRNA
PD-L1 protein & PD-L1 mRNA
PD-1 protein & PD-1 mRNA
PD-L1 mRNA & PD-1 mRNA
PD-L1 protein & PD-1 protein
PD-L1 mRNA & PD-1 protein
PD-L1 protein & PD-1 mRNA
PD-L1 mRNA & PD-1 protein & PD-1 mRNA
PD-L1 protein & PD-1 protein & PD-1 mRNA
PD-L1 protein & PD-L1 mRNA & PD-1 protein
PD-L1 protein & PD-L1 mRNA & PD-1 mRNA
All four biomarkers

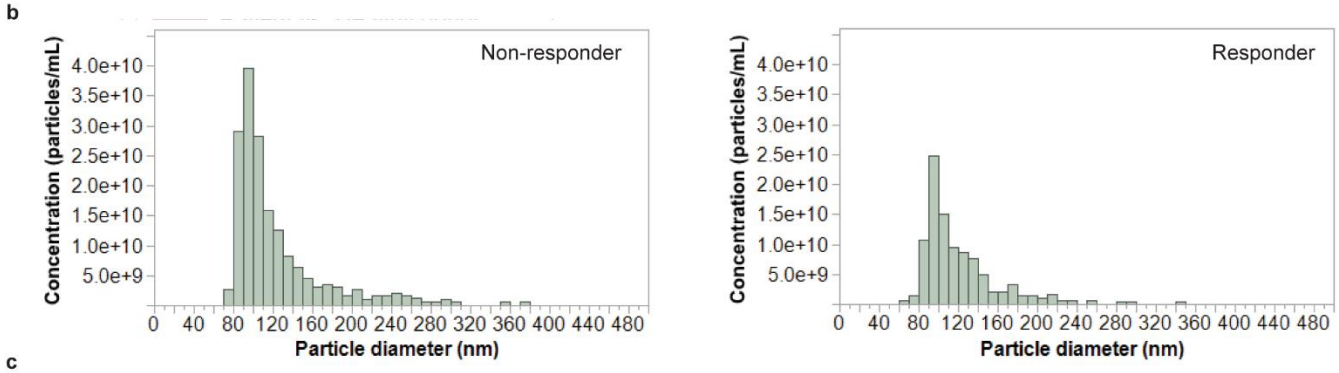
b
Non-responder
Responder
Concentration (particles/mL)
4.0e+10
3.5e+10
3.0e+10
2.5e+10
2.0e+10
1.5e+10
1.0e+10
5.0e+9
0 40 80 120 160 200 240 280 320 360 400 440 480
Particle diameter (nm)

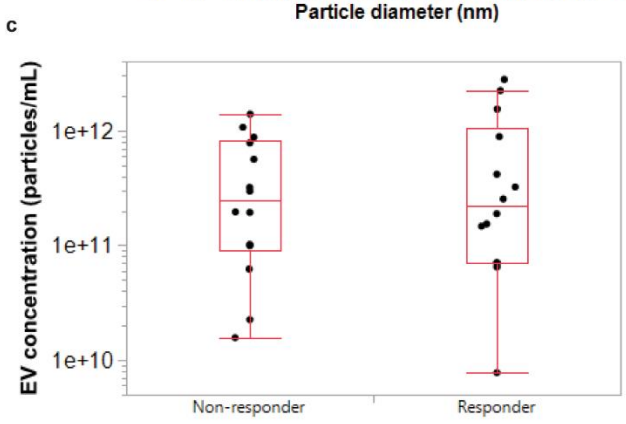
c
EV concentration (particles/mL)
1e+12
1e+11
1e+10
Non-responder
Responder

Figure S16. Characterization of EVs from the serum of non-responders (n = 27) and responders (n = 27). **a** Area under the curve (AUC) values of receiver operating characteristic (ROC) curve analyses for the single-EV immunotherapy biomarkers measured with ^{Au}SERP. For NSCLC diagnosis, the sample size consisted of patients (n = 54) vs. healthy donors (n = 20). For prediction of NSCLC patient response to anti-PD-1/PD-L1 immunotherapy, the sample size consisted of responders (n = 27) vs. non-responders (n = 27). An ROC curve analysis was performed for a single biomarker and multiple biomarkers with different permutations. **b** Representative size distributions of the patient serum-derived EVs measured with TRPS. **c** Box plots of the concentrations of the patient serum-derived EVs measured with TRPS.

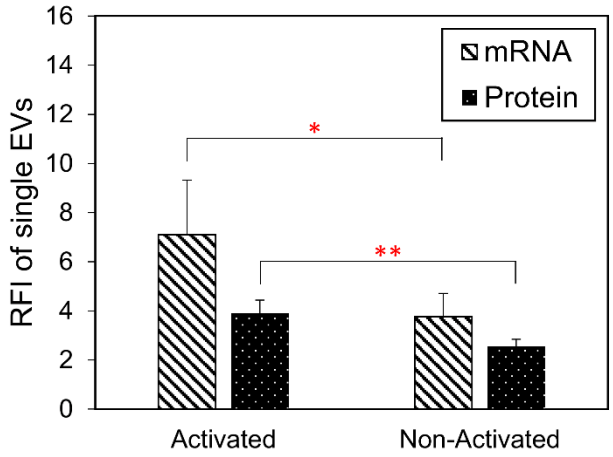

Figure S17. ^{Au}SERP distinguishes T-cell status via single-EV PD-1 levels. EVs from activated and non-activated T cells were harvested after 3 days and screened with ^{Au}SERP for PD-1 protein and mRNA levels. (*p < 0.05, **p < 0.01, Student's t-test). The data were expressed as mean ± SD; n = 3. RFI, relative fluorescence intensity.

Table S1. Clinical characteristics of stage IV NSCLC patients.

	Non-responder (n= 27)	**Responder (n = 27)**
Age		
Median (range)	63 (47 – 83)	65 (45 – 86)
Gender		
Male	14	18
Female	13	9
Race		
Caucasian	23	24
African American	4	3
Smoking history		
Current	7	6
Former	19	21
Never	1	0
Performance status		
0	5	6
1	18	19
2	4	2
Histology		
Adenocarcinoma	19	18
Squamous cell	7	5
Adenosquamous	0	1
NOS	1	3
PD-L1 IHC		
Positive	12	17
Negative	6	4
Unknown	9	6
EGFR		
Wild	18	22
Mutant	5	1
Unknown	4	4
Drug		
Nivolumab	20	17
Pembrolizumab	7	9
Atezolizumab	0	1

Table S2. Detailed information on the patients enrolled in the study.

ID	Response	PD-L1 IHC	Age	Gender	Race	Smoking history	Performance status	Treatment
N001	Non-responder	Negative	70	Male	Caucasian	Former	1	Nivolumab
N002	Non-responder	Negative	77	Female	Caucasian	Current	1	Nivolumab
N003	Non-responder	Negative	62	Male	Caucasian	Former	0	Nivolumab
N004	Non-responder	Negative	51	Male	African American	Former	0	Pembrolizumab
N005	Non-responder	Negative	61	Male	Caucasian	Former	0	Nivolumab
N006	Non-responder	Negative	47	Female	Caucasian	Current	1	Nivolumab
N007	Non-responder	Positive	71	Female	Caucasian	Former	1	Nivolumab
N008	Non-responder	Positive	69	Female	Caucasian	Former	1	Nivolumab
N009	Non-responder	Positive	64	Male	Caucasian	Former	1	Nivolumab
N010	Non-responder	Positive	83	Male	Caucasian	Former	0	Nivolumab
N011	Non-responder	Positive	68	Female	Caucasian	Former	1	Nivolumab
N012	Non-responder	Positive	82	Female	Caucasian	Former	1	Pembrolizumab
N013	Non-responder	Positive	56	Male	Caucasian	Former	1	Pembrolizumab
N014	Non-responder	Positive	63	Male	Caucasian	Former	1	Pembrolizumab
N015	Non-responder	Positive	56	Female	African American	Current	2	Pembrolizumab
N016	Non-responder	Positive	58	Male	African American	Current	1	Pembrolizumab
N017	Non-responder	Positive	66	Female	Caucasian	Never	1	Pembrolizumab
N018	Non-responder	Positive	63	Male	Caucasian	Former	2	Nivolumab
N019	Non-responder	Unknown	65	Female	Caucasian	Former	1	Nivolumab
N020	Non-responder	Unknown	51	Male	Caucasian	Former	2	Nivolumab
N021	Non-responder	Unknown	70	Female	Caucasian	Former	0	Nivolumab
N022	Non-responder	Unknown	58	Female	Caucasian	Current	1	Nivolumab

N023	Non-responder	unknown	54	Female	Caucasian	Current	2	Nivolumab
N024	Non-responder	Unknown	50	Female	Caucasian	Former	1	Nivolumab
N025	Non-responder	Unknown	57	Male	African American	Former	1	Nivolumab
N026	Non-responder	Unknown	74	Male	Caucasian	Former	1	Nivolumab
N027	Non-responder	Unknown	56	Male	Caucasian	Current	1	Nivolumab
R028	Responder	Negative	70	Male	Caucasian	Former	1	Nivolumab
R029	Responder	Negative	65	Male	Caucasian	Former	0	Nivolumab
R030	Responder	Negative	83	Male	Caucasian	Former	1	Pembrolizumab
R031	Responder	Negative	63	Female	Caucasian	Current	1	Nivolumab
R032	Responder	Positive	76	Female	African American	Former	1	Nivolumab
R033	Responder	Positive	45	Female	African American	Current	1	Nivolumab
R034	Responder	Positive	69	Male	Caucasian	Former	1	Nivolumab
R035	Responder	Positive	51	Male	Caucasian	Current	1	Atezolizumab
R036	Responder	Positive	62	Male	Caucasian	Former	1	Nivolumab
R037	Responder	Positive	86	Male	Caucasian	Former	1	Nivolumab
R038	Responder	Positive	63	Female	Caucasian	Former	1	Nivolumab
R039	Responder	Positive	57	Female	Caucasian	Former	1	Nivolumab
R040	Responder	Positive	75	Male	African American	Former	2	Pembrolizumab
R041	Responder	Positive	55	Male	Caucasian	Former	0	Pembrolizumab
R042	Responder	Positive	59	Male	Caucasian	Former	0	Pembrolizumab
R043	Responder	Positive	62	Male	Caucasian	Former	0	Pembrolizumab
R044	Responder	Positive	65	Female	Caucasian	Former	1	Pembrolizumab
R045	Responder	Positive	72	Male	Caucasian	Former	1	Pembrolizumab
R046	Responder	Positive	71	Male	Caucasian	Former	1	Pembrolizumab
R047	Responder	Positive	67	Male	Caucasian	Current	1	Nivolumab

R048	Responder	Positive	66	Female	Caucasian	Former	1	Pembrolizumab
R049	Responder	Unknown	65	Female	Caucasian	Current	0	Nivolumab
R050	Responder	Unknown	60	Female	Caucasian	Former	1	Nivolumab
R051	Responder	Unknown	73	Male	Caucasian	Former	2	Nivolumab
R052	Responder	Unknown	51	Male	Caucasian	Current	1	Nivolumab
R053	Responder	Unknown	58	Male	Caucasian	Former	0	Nivolumab
R054	Responder	Unknown	65	Male	Caucasian	Former	1	Nivolumab

Table S3. Average values for the performances of ELISA and ^{Au}SERP at detecting EV PD-L1 protein. NA, not applicable; ND, not detected.

Number of spiked tumor EVs	TFI of single EVs (a.u.)	PD-L1 concentration (pg/mL)
2.00E+10	Single-EV NA	13.79
1.00E+10	Single-EV NA	6.90
4.00E+09	Single-EV NA	2.11
1.00E+09	240000000	1.33
2.00E+08	217000000	0.31
4.00E+07	129000000	ND
8.00E+06	67100000	ND
1.60E+06	28500000	ND
3.20E+05	8070000	ND

Table S4. Average values for the performances of qRT-PCR and ^{Au}SERP at detecting EV PD-L1 mRNA. NA, not applicable; ND, not detected.

Number of spiked tumor EVs	TFI of single EVs (a.u.)	Cycle Threshold (Ct)
4.00E+10	Single-EV NA	28.09
5.00E+09	Single-EV NA	37.26
1.00E+09	14054377	39.13
2.00E+08	8508105	ND
4.00E+07	3406813	ND
8.00E+06	1145519	ND
1.60E+06	663258	ND
3.20E+05	415275	ND
6.40E+04	359476	ND

Table S5. Antibodies used for single-EV capture and detection.

Antibody		**Catalog number/ Brand name**	**Supplier**
Capture	CD63	MAB5048	R&D Systems
	CD9	MAB1880	R&D Systems
	EGFR (Cetuximab)	Erbitux®	ImClone LLC
	EpCAM	AF960	R&D Systems
	CD3	MAB100100	R&D Systems
	Biotinylated CD4	344610	BioLegend
	Biotinylated CD8	344720	BioLegend
Detection	CD63 - Alexa Fluor® 488	sc-5275 AF488	Santa Cruz Biotechnology
	PD-L1	86744S	Cell Signaling Technology
	PD-L1	ab205921	Abcam
	PD-1	86163S	Cell Signaling Technology